LA-UR-98-1902
March 1998

THERMAL AND FLOW ANALYSIS OF THE FLUOR DANIEL, INC., NUCLEAR MATERIAL STORAGE FACILITY RENOVATION DESIGN (INITIAL 30% EFFORT OF TITLE I)

by

Robert G. Steinke, Cathrin Müller, and Thad D. Knight

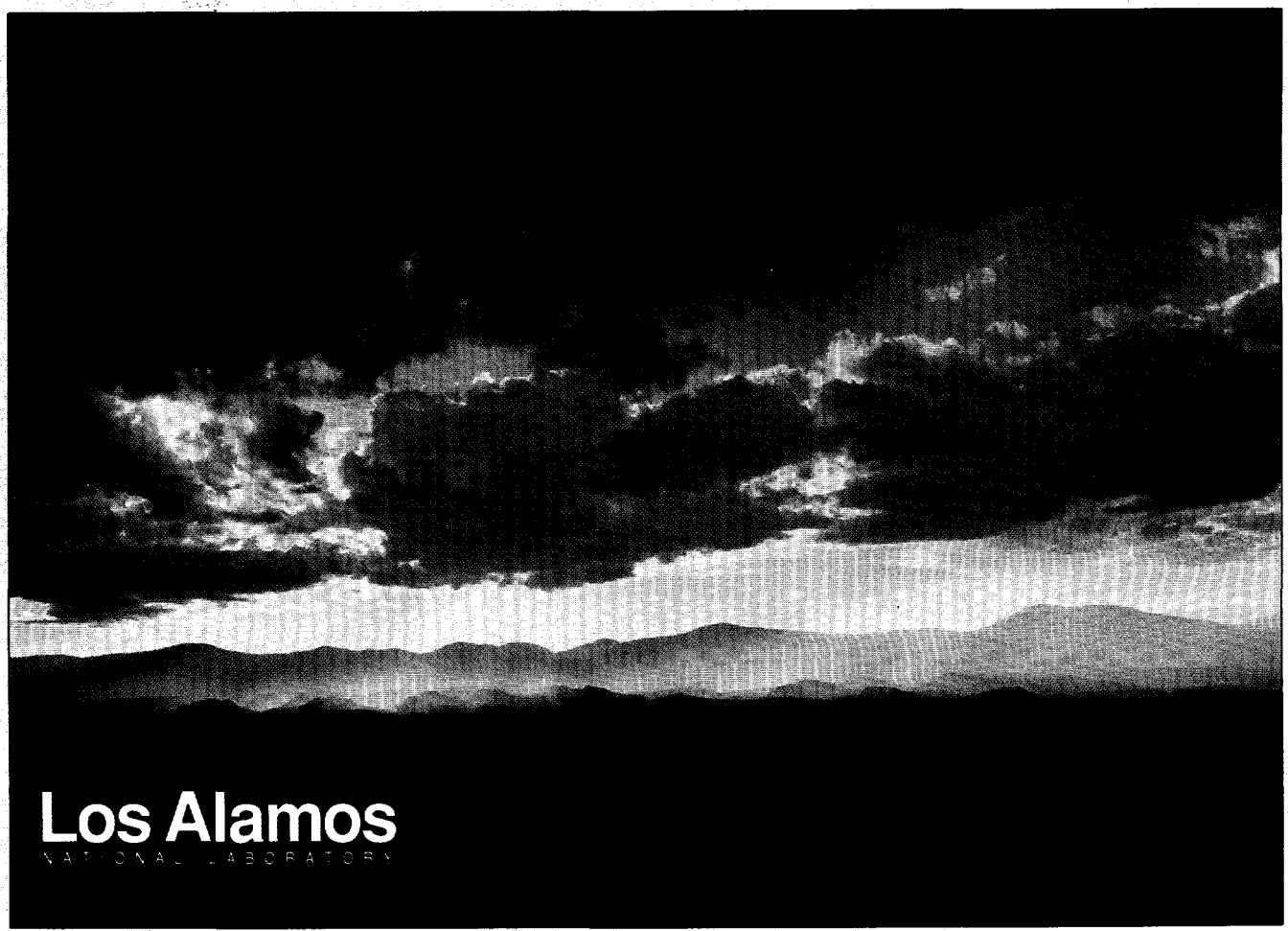

Photograph: by Chris J. Lindberg

DISCLAIMER

LA-UR-98-1902

THERMAL AND FLOW ANALYSIS OF THE FLUOR DANIEL, INC., NUCLEAR MATERIAL STORAGE FACILITY RENOVATION DESIGN (INITIAL 30% EFFORT OF TITLE I)

by

Robert G. Steinke, Cathrin Müller, and Thad D. Knight

ABSTRACT

The computational fluid dynamics code CFX4.2 was used to evaluate steady-state thermal-hydraulic conditions in the Fluor Daniel, Inc., Nuclear Material Storage Facility renovation design (initial 30% of Title I). Thirteen facility cases were evaluated with varying temperature dependence, drywell-array heat-source magnitude and distribution, location of the inlet tower, and no-flow curtains in the drywell-array vault. Four cases of a detailed model of the inlet-tower top fixture were evaluated to show the effect of the canopy-cruciform fixture design on the air pressure and flow distributions.

1.0. INTRODUCTION

Fluor Daniel, Inc., has provided a Nuclear Material Storage Facility (NMSF) renovation design for analysis during the initial 30% effort of Title I (also referred to as the 30% NMSF design). Group TSA-10 at Los Alamos National Laboratory (LANL) has analyzed that design for the air-temperature and air-flow conditions in the facility and for drywells that stage special nuclear material in double- or triple-can storage containers. Stored plutonium generates heat (from alpha-particle decay) that is removed by conduction, convection, and radiation heat transfer from the plutonium, cans, drywell, and facility. The design must provide good heat-transfer paths that keep the maximum plutonium temperature as low as possible below specified temperature limits for different forms of plutonium.

This report discusses the results from analyzing (1) variations in a numerical model of the facility and (2) a detailed numerical model of the cruciform and canopy top of the inlet tower. During the 30% to 60% effort of Title I, we will investigate further variations on these models and a detailed numerical model of the top shroud of the outlet stack and a numerical model of the drywell, which has a fixture that supports the storage containers. Some design parameters for these later models are preliminary at this time. This report also notes temperature results from the analysis of earlier drywell models to provide a current estimate of the peak plutonium-metal temperature using the facility-analysis results of this report.

2.0. FACILITY ANALYSES

The CFX4.2 three-dimensional (3D), computational fluid-dynamics (CFD) computer program, developed by AEA Technology, was used to model the 30% NMSF design. Air flow through the facility is driven by the buoyancy force of natural convection created by the drywell-array heatup of the vault air. The facility design is a passive system for heat removal.

2.1. Facility Model

The following information was used to create two facility models for the inlet tower, drywell-array vault, and outlet stack 1 with CFX4.2 MeshBuild:

1. The 30% NMSF design drawings from Fluor Daniel, Inc., dated March 7, 1998, and

2. E-mail and telephone conversations,[1] which clarified and corrected some design parameters in the drawings.

One model has the inlet tower on the inlet-end side of the vault, as shown in the drawings. The second model, which has the inlet tower relocated to the inlet-end end of the vault, is a mirror image of the inlet tower, drywell-array vault, and outlet stack 2. The purpose of the second model is to investigate the inlet air-flow difference when the inlet tower is moved from the inlet side to the inlet end of the drywell-array vault.

The air volume inside the inlet tower, drywell-array vault, and outlet stack 1 was modeled with 63 connecting 3D block volumes. Each block was overlaid with a mesh-cell grid that has continuity of the mesh across the block-connecting faces. Mesh-cell dimensions in the three Cartesian-coordinate directions range from 3.8 to 12.6 in. The first model (with the inlet tower on the side) has a total of 126,860 mesh cells, whereas the second model has a total of 120,588 mesh cells. There are fewer mesh cells in the second model because in relocating the inlet tower, the number of mesh cells across the inlet tower in one horizontal direction needed to be reduced from 16 to 12 to be consistent with the 12 mesh cells across the drywell-array vault.

A grille (screen) having 1-in.-pitch square holes and a security grate having 6-in.-pitch square holes were modeled at the inlet/outlet boundary faces and internally at the concrete-foundation bases, respectively, of the metal inlet tower and outlet stack. The drywell array in each vault has 47 rows of drywells down the vault and 4 drywells per row across the vault in a 30-in.-pitch inline array of 18-in. outer-diameter drywells.

Two cases of adding no-flow vertical curtains across the drywell-array vault are modeled as an assumed aid to directing air flow vertically and avoiding possible air-flow-swirl hot spots during the initial loading. These curtains are not in the 30%

NMSF design. They are a possible design variation that we felt was important to consider.

2.2. Thermal-Hydraulic Model

CFX4.2 Solver was used to evaluate a steady-state calculation of the internal-air thermal-hydraulic state in the CFX4.2 MeshBuild model. This evaluation was performed in 3D Cartesian coordinates with a body-fitted grid, a turbulence k-ε model, convective heat transfer, adiabatic exterior walls, wall drag, a drywell-array porous region, a drywell-array 3D volumetric heat source, and atmospheric-pressure boundary conditions at the top of the inlet tower and outlet stack. The air density was modeled as either incompressible (where the air density is constant, except in the gravity-head buoyancy term, where the Boussinesq approximation defines air-density temperature dependence) or weakly compressible (where air-density temperature dependence is defined in all terms of the conservation equations by the air ideal-gas equation of state) at the LANL reference atmospheric pressure of 76,976 Pa = 11.16 psia. The inlet air temperature was assumed to be 308.15 K = 95.0°F.

Iterative convergence of the steady-state solution was based on the premise that

1. air mass flow in equals air mass flow out,
2. air enthalpy in plus the drywell-array heat source equals air enthalpy out,
3. the absolute value of the air-mass-flow residual summed over all mesh cells divided by the air mass flow through the facility is $\sum|\Delta\dot{m}|/\dot{m} < 0.001$, and
4. the absolute value of the air-enthalpy residual summed over all mesh cells divided by the drywell-array heat source is $\sum|\Delta(\dot{m}\cdot e)|/(\text{heat source}) < 0.001$.

AEA Technology, the developer of CFX4.2, claims that there is sufficient steady-state iterative convergence when the values of the later two criteria are <1% (0.01).

The air-flow resistance of the inlet/outlet grille and grate and the vault drywell array were modeled by the CFX4.2 body-force $\Delta P/L = B + (R_c + R_f\cdot|V|)\cdot V$, where ΔP is the pressure loss over the air-flow length L for an air velocity of V and B, R_c, and R_f are input constants. The B, R_c, and R_f values were determined by fitting the CFX4.2 body-force formula to K-factor correlation formulas in Idelchik.[2] The grille and grate K-factor formulas gave $\Delta P/L = C\cdot V^2$ for an exact fit with $B = 0$, $R_c = 0$, and $R_f = C$. The drywell-array K-factor formula gave $\Delta P/L = C\cdot V^{1.8}$, which was approximated with $B = 0$ and R_c and R_f determined by fitting $\Delta P/L = B + (R_c + R_f\cdot|V|)\cdot V$ to $\Delta P/L = C\cdot V^{1.8}$. The fit was done at $V = 0.1$ m s^{-1} and $V = 0.2$ m s^{-1} for air flow down the vault and at $V = 0.02$ m s^{-1} and $V = 0.04$ m s^{-1} for air flow across the vault. $V = 0.16$

$m\ s^{-1}$ is the average air-flow velocity down the vault for a single-vault volumetric air flow of 5000 $ft^3\ min^{-1}$. No drywell air-flow resistance is modeled in the vertical direction to compensate for not modeling the effect of concentrated heating in the drywell outer-surface boundary layer on the vertical buoyancy force with a porous-region model.

The magnitude and 3D distribution of the drywell-array heat source and other design features were varied among the following 13 cases evaluated by CFX4.2 Solver:

1. 10,000 W—Constant 16.246-W m^{-3} heat source in the drywell-array volume and an incompressible-flow constant air density;

2. 10,000 W—Case 1, with incompressible flow replaced by weakly compressible flow (all subsequent cases use a weakly compressible flow that has an air density with temperature dependence);

3. 10,005 W—Case 2, with the constant heat source replaced by a realistic heat source having a uniform distribution of three or four heated cans per drywell (axially distributed at can locations 3, 8, and 13 or 2, 6, 10, and 14) in a horizontal-plane checkerboard pattern, with a 14.8-in. vertical spacing between can locations;

4. 10,005 W—An inlet-end loading requested by Fluor Daniel, Inc., with drywell rows 1 to 16 having 4 drywells with 10 heated cans, and drywell row 17 having 1 drywell with 10 heated cans and 1 drywell with 7 heated cans, with a 16.0-in. vertical spacing between can locations;

5. 19,995 W—Similar to Case 4, having double the heat source, with drywell rows 1 to 33 having 4 drywells with 10 heated cans and drywell row 34 having 1 drywell with 10 heated cans and 1 drywell with 3 heated cans, with a 16.0-in. vertical spacing between can locations;

6. 10,005 W—Similar to Case 4, having 20% of the heat load at the inlet end and 80% at the outlet end of the drywell-array vault, with drywell rows 1 to 3 having 4 drywells with 10 heated cans, drywell row 4 having 1 drywell with 10 heated cans and 1 drywell with 3 heated cans, drywell row 34 having 1 drywell with 10 heated cans and 1 drywell with 4 heated cans, and drywell rows 35 to 47 having 4 drywells with 10 heated cans, with a 16.0-in. vertical spacing between can locations;

7. 7575 W—Similar to Case 6, having a loading of 2.5 tonnes rather than 3.3 tonnes of plutonium in the vault, with drywell rows 1 to 2 having 4 drywells with 10 heated cans, drywell row 3 having 2 drywells with 10 heated cans and 1 drywell with 1 heated can, drywell row 37 having 1 drywell with 4 heated cans, and drywell rows 38 to 47 having 4 drywells, with 10 heated cans, with a 16.0-in. vertical spacing between can locations;

8. 10,005 W—Case 4, with the inlet tower moved from the side to the end of the drywell-array-vault inlet, giving a model that is a mirror image of the inlet tower, drywell-array vault, and outlet stack 2;

9. 10,005 W—A nonuniform heat-source version of Case 3, with the heat source concentrated at the vertical center of the drywell-array vault at can locations 6, 7, 8, 9, and 10, with drywell rows 1 to 8, 13 to 28, and 37 to 45 having 4 drywells with 5 heated cans and drywell row 46 having 1 drywell with 5 heated cans and 1 drywell with 2 heated cans, with a 14.8-in. vertical spacing between can locations;

10. 10,005 W—Case 9, with no-flow vertical curtains every 4 drywell rows across the vault and from 6 ft to 12 ft, 6 in. above the vault floor;

11. 10,005 W—Case 9, with the horizontal heat source of each drywell changed from a uniform distribution in its 3 x 3 cell area to being concentrated in the center cell as a better approximation of the concentrated heat source of the drywell outer-surface boundary layer;

12. 600 W—Derived from Case 11, having only 6% of the design heat load, with drywell rows 16 and 32 having 4 drywells with 5 heated cans, with a 14.8-in. vertical spacing between can locations; and

13. 10,005 W—Case 10, with curtains every 2 rather than 4 drywell rows; curtains 9 ft, 6 in. rather than 6 ft, 6 in. tall; and curtains with their bottom edge starting 7 ft, 3 in. from the vault floor and decreasing 3 in. with each curtain to 1 ft, 9 in. from the vault floor for the last curtain. The sloped inlet ceiling and sloped outlet floor were eliminated, and the drywell heat source was concentrated in its center cell, as in Cases 11 and 12.

The differences between the following cases investigate the effects of

- Cases 1 and 2—air-density temperature dependence in all equation terms,
- Cases 2 and 3—constant vs realistic uniform heat-source distribution,
- Cases 4, 5, 7, and 12—magnitude of the drywell-array total heat source,
- Cases 3, 4, 6, and 9—distribution of the drywell heat source down the vault,
- Cases 2, 3, 4, and 9—distribution of the drywell heat source vertically,
- Cases 4 and 8—location of the inlet tower at the side or end of the vault inlet,

- Cases 9 and 11—concentration of the drywell heat source in its center cell, and

- Cases 9, 10, and 13—curtains redirecting the vault air flow vertically.

The vertical-distribution volumetric heat source of each drywell is defined by the drywell outer-surface integrated heat flux from a CFX steady-state drywell calculation. Each such calculation is unique for the vertical can locations having heated cans and the vertical spacing between cans in the drywell. The above 13 cases require 4 drywell calculations (2, 3, 4, or 5 heated cans) with 14.8-in. vertical spacing and 5 drywell calculations (1, 3, 4, 7, or 10 heated cans) with 16.0-in. vertical spacing between cans. Performing those drywell calculations with conduction, convection, and radiation heat transfer would require an effort similar to performing the above facility calculations. Those drywell calculations were not performed at this time. Instead, each vertical-distribution volumetric heat source was approximated by adding together the vertical-distribution heat source from a single heated can (evaluated a year ago) for each heated can in the drywell at its stated vertical location. This approximation has been shown to be reasonably accurate when compared to the vertical-distribution volumetric heat source from several multiple-heated-can drywell calculations.

2.3. Analysis Results

CFX4.2 View plots of the air temperature, pressure, and speed results from the 13 facility calculations by CFX4.2 Solver have been documented.[3,4] A summary of those results is shown in Table I. Comparison of the solution results from the following cases showed the following.

- Cases 1 and 2 (incompressible vs weakly compressible)—The air pressure-distribution results are somewhat different, whereas the air flow and temperature results are approximately the same. We expect the weakly compressible results to be more accurate. The weakly compressible pressure distribution appears to be acceptable, whereas the incompressible pressure-distribution defining form appears to be different from what is expected. The inlet-tower top air-inflow distribution has a difference that may be caused by the weakly compressible pressure being a static pressure and the incompressible pressure being a dynamic (static plus kinetic) pressure. A constant real (dynamic) pressure boundary condition appears to be needed in the weakly compressible calculation to give the correct inlet-tower top air-inflow distribution that was determined by the incompressible calculation.

- Cases 2 and 3 (constant vs realistic uniform heat-source distribution)—Modeling a realistic heat-source distribution from uniformly distributed heated cans causes the maximum air temperature at can locations 13 and above in the last seven drywell rows to be ~1.0 K (1.8°F) hotter.

TABLE I
RESULTS FROM THE CASES MODELED AND EVALUATED BY CFX4.2 FOR THE 30% NMSF DESIGN

Case Number	Heat Source (W)	Volumetric Air Flow ($ft^3\ min^{-1}$)	Maximum Air Temperature (K, °F)		$P - P_{ref} - \rho_{inlet} \cdot g \cdot z$ Pressure Range (Pa)
1	10,000	5490	313.34	104.34	-3.2757 to 0.0153
2	10,000	5514	313.23	104.14	-4.1755 to 0.1074
3	10,005	5505	314.28	106.03	-4.1969 to 0.1075
4	10,005	5479	313.35	104.36	-4.0661 to 0.1078
5	19,995	6812	316.13	109.36	-5.8354 to 0.0944
6	10,005	5466	313.18	104.05	-4.0368 to 0.1079
7	7575	5008	313.18	104.05	-3.5259 to 0.1127
8	10,005	5522	313.31	104.29	-4.1007 to 0.1102
9	10,005	5389	314.54	106.50	-4.2224 to 0.1087
10	10,005	4685	316.08	109.27	-4.2448 to 0.1156
11	10,005	5380	314.59	106.59	-4.2167 to 0.1085
12	600	2289	310.29	98.85	-1.3981 to 0.1785
13	10,005	3965	316.39	109.83	-4.2653 to 0.1231

- Cases 4, 5, 7, and 12 (total heat source varied)—The inlet volumetric air flow and air temperature as a function of the drywell-array total heat source from these four cases in Table I can be predicted reasonably by the following least-squares-fit functional forms:

  volumetric air flow ($ft^3\ min^{-1}$) = 255.2 x [heat source (W)]$^{1/3}$, and
  air temperature (°F) = 95.0 + 0.1037 x [heat source (W)]$^{1/2}$.

  All of these cases have a similar air-flow pattern, with less air flow per unit of heat source as the heat-source magnitude is increased so that the initial loading of the vault is better cooled.

- Cases 3, 4, 6, and 9 (down-the-vault heat-source distribution varied)—With a uniform air flow directed down the drywell-array vault, the drywells with the last heated cans experience the vault's maximum air temperature. Drywell rows must have heated cans loaded uniformly across the vault so that the full cross section of uniform air flow experiences the same heating. When this is done, loading the last heated drywell near the inlet, middle, or outlet of the vault causes it to experience the same maximum air temperature.

- Cases 2, 3, 4, and 9 (vertical heat-source distribution varied)—The vault's maximum air temperature at the location of heated cans is less when the heated cans are loaded in the vertical bottom and middle can locations of the drywell. Heated cans should not be loaded in the top 20% of the drywell in the inlet half because of less air flow (see Fig. 1) or in the outlet half because of hotter air temperatures near the ceiling in Cases 2 and 3.

- Cases 4 and 8 (inlet tower at the side or end of the vault inlet)—Air flow is slightly higher, and the maximum air-temperature change is slightly lower (both <1%) when the inlet tower is at the end rather than the side of the vault inlet. With the inlet tower at the side, the air flow swirls primarily horizontally, whereas at the end, the air flow swirls primarily vertically under the inlet sloped ceiling, as shown in Figs. 1 and 2.

- Cases 9 and 11 (concentrate the heat source in the drywell center cell)—There is a negligible difference in the solution when concentrating the drywell heat source in the center cell of the drywell's 3 x 3 cell area. A slightly hotter localized heating of the air occurs in the temperature plots at the location of each drywell.

- Cases 9, 10, and 13 (curtains in the drywell-array vault)—Curtains every two or four drywell rows are not close enough to prevent air-flow swirls between curtains. The vertical air flow is of the same magnitude as the swirls. There is an undesirable vertical and swirl air flow of a lesser magnitude between curtains with unheated drywells. The added air-flow resistance of curtains every two or four drywell rows reduces the volumetric air flow by 26% or 13% and increases the maximum air-temperature change by 29% or 24%, respectively.

2.4. Significant Findings

Analyzing the thermal-hydraulic solution results from the 13 facility cases in Refs. 2 and 3 gave the following significant findings:

1. The Fluor Daniel renovation design provides a uniform air-flow distribution across the drywell-array vault that remains unchanged as the air flows down the vault.

2. The vault inlet has a horizontal air-flow swirl with the inlet tower on the side and a vertical air-flow swirl with the inlet tower on the end (there also is a lesser vertical air-flow swirl near the inlet-tower-side vault wall, with the inlet tower on the side and a lesser horizontal air-flow swirl near the top of the sloped inlet ceiling, with the inlet tower on the end; see Figs. 1 and 2).

3. The sloped inlet ceiling and outlet floor help to distribute air flow uniformly across the drywell array; however, some of the inlet air-flow swirl affects the first row of drywells (see Figs. 1 and 2).

4. Volumetric air flow through the facility with a varying heat source was found to be approximated reasonably by the least-squares-fit functional-form volumetric air flow ($ft^3\ min^{-1}$) = 255.2 x [heat source (W)]$^{1/3}$ so that a lesser total heat source provides more air flow per unit heat source for cooling the heated drywells.

5. Incompressible vs weakly compressible modeling of the air density gave the same air flow and temperature results; however, there appears to be a different defining form for the CFX relative pressure so that a dynamic- rather than static-pressure boundary condition appears to be needed in a weakly compressible calculation.

6. With uniform air flow across the drywell array vault, drywells across the vault must have the same heat loading to provide a uniform heating of the air that minimizes the vault's maximum air temperature.

7. With a uniform heat source across the vault, the last heated drywell down the vault experiences the vault maximum air temperature (see Fig. 3).

8. Heated cans (with maximum-temperature-limited plutonium metal) should be loaded in the lower 80% of the drywell because of lower air flow in the inlet half and warmer air progressively accumulating near the ceiling in the outlet half of the drywell-array vault.

9. Concentrating the drywell heat source in the center cell of the 3 x 3 cell horizontal-plane area of each drywell appears to have little effect on the thermal-hydraulic solution but is a better modeling approximation of the concentrated heating of the drywell outer-surface boundary layer.

10. For a volumetric air flow through the facility of <5000 $ft^3\ min^{-1}$ (Cases 10, 12, and 13), an air back-flow swirl occurs at the inlet-tower side of the beveled top of the outlet stack; this may occur because the inner-diameter change from 5 ft to 6.5 ft over a 5-ft height is too large an expansion of the flow area.

11. The ratio of the maximum air-temperature change to the ideal uniform-heating-of-the-air air-temperature change was 1.12 to 1.17 for Cases 5, 6, 2, 1, 4, and 8; 1.34 to 1.42 for Cases 13, 7, 3, 9, and 11; 1.53 for Case 10; and 3.35 for Case 12; thus, the Fluor-Daniel design with the heated cans in the bottom 10 can locations appears to provide the most efficient heating of the air.

12. Using curtains in the drywell-array vault to establish vertical air flow only for the heated drywells is not a viable concept for this facility design because of the additional air-flow resistance from the curtains and the air-flow swirls between curtains and the bypass air flow for the unheated drywells.

13. Considering Cases 3 through 9, 11, and 12 with different heat-source distributions in the Fluor-Daniel facility design, the maximum air-temperature rise in the drywell-array vault is 11.6°F (6.4 K) from Case 11 for a 10,005-W heat source and 14.4°F (8.0 K) from Case 5 for a 19,995-W heat source.

3.0. INLET-TOWER FIXTURE ANALYSES

3.1. Geometry Model

According to the 30% NMSF design drawings from Fluor Daniel, Inc., the inlet-tower top fixture consists of a canopy, cruciform, and grilles (screens) on all four sides of the tower underneath the canopy. This basic design was varied to show the effects of the canopy and cruciform and the effect of the addition of the grilles in terms of the resulting pressure difference.

The inlet-tower fixture was surrounded by an extended region of air to minimize the effect of the domain boundaries on air flow in the tower. The computational domain extends three times the tower width to the sides and top from the fixture. The bottom boundary models only the top half of the inlet tower, which is above the building. The domain was modeled with 18 connecting 3D block volumes. A nonuniform Cartesian grid was created across all blocks with 100,000 mesh cells. Mesh-cell dimensions range from 0.1 m (4 in.) in the tower and below and above the canopy to 1.3 m (52 in.) at the outer edges of the domain.

The canopy and cruciform were modeled as no-flow interfaces, and the grilles, with assumed 1-in.-pitch square holes, were modeled by one-cell-thick mesh-cell planes with air-flow resistance, as discussed in Sec. 2.2.

3.2. Thermal-Hydraulic Model

CFX4.2 Solver was used to evaluate a steady-state calculation of the air thermal-hydraulic state inside the inlet-tower fixture.

Four different cases were evaluated.

Case 1: Inlet tower without canopy, cruciform, and grilles and no wind.

Case 2: Inlet tower with canopy and cruciform, without grilles, and no wind.

Case 3: Inlet tower with canopy, cruciform, and grilles and no wind.

Case 4: Inlet tower with canopy, cruciform, and grilles and with a horizontal wind parallel to one direction.

The model had a 3D rectangular grid and was isothermal and incompressible. The k-ε turbulence model was used.

The initial conditions were an air density of 0.87023 kg m^{-3}, an air temperature of 308.15 K (95°F), and an air pressure of 76976 Pa. These numbers were selected to be consistent with the initial conditions for the facility model, as discussed in Sec. 2.2.

For the first three cases (no wind), all sides of the computational domain and the top were specified with atmospheric-pressure boundary conditions. For the inlet-tower outlet (bottom of the tower in the model), a mass-flow boundary condition was used with a volumetric air flow of 5500 ft^3 min^{-1} that corresponds to the air flow from the facility model. The remaining bottom of the domain also was an atmospheric-pressure boundary.

In Case 4, the same volumetric air-flow boundary condition was used for the inlet-tower outlet. An atmospheric-pressure boundary condition was used on the top and sides where no wind was coming in. The horizontal wind came directly from the west boundary, with a constant velocity of 7.5 m s^{-1} (16.8 mph). This velocity was taken from Ref. 5 and is common during the spring in Los Alamos. The existing pressure boundary condition takes only static pressure into account and not the dynamic pressure created by the wind. Because of this, we saw nonphysical behavior on the bottom boundary when specified as an atmospheric-pressure boundary. Eventually, this boundary was modeled as a free-slip wall, meaning that there was no shear in either direction parallel to the wall, and air flow would go across it without resistance.

Because of the isothermal nature of the analyses for the inlet-tower fixture, iterative convergence of the steady-state solution was based on criteria 1 and 3, as discussed in Sec. 2.2.

3.3. Analysis Results

Air pressure and speed results are documented in a series of CFX4.2 View plots.[6] A summary of those results is shown in Table II.

In all three no-wind cases, the maximum negative pressure is generated at the tower entrance, where the air flows around a sharp corner. There are almost no differences between Cases 1 and 2. By adding the grilles, the pressure difference across the tower height and the maximum velocity inside the tower increase. For actual air pressure contours and speed vectors from Case 3, see Figs. 4 and 5.

TABLE II
RESULTS FROM CASES FOR THE INLET-TOWER FIXTURE

Case Number	Change in Pressure from Inlet to Outlet (Pa)	Maximum Velocity in the Inlet Tower and Fixture ($m\ s^{-1}$)
1	-0.162	0.594
2	-0.169	0.595
3	-0.211	0.698
4	6.71	6

In Case 4, we observed counter-current air flow in the tower. Air flowed around the bottom of the cruciform and into a vertical vortex on the far side of the cruciform from the wind. Some air flowed down the tower, but much of it flowed out through the grilles.

4.0. DRYWELL-CONTAINER ANALYSES

A complete thermal analysis of the facility is necessary to couple the facility model (which determines the air-temperature change from ambient to the drywell-array vault maximum) with a drywell model (which determines the air-temperature change from the drywell-array vault maximum to the plutonium maximum) under worst-case conditions. The facility model requires vertical heat-flux distributions from the outer surface of different drywells as its volumetric heat-source boundary condition, whereas the drywell model requires the vault vertical air-temperature and air-flow distributions at its drywell-array location as its boundary conditions. A few iterations between these models may be required for consistency of the heat-flux, air-temperature, and air-flow solutions.

A drywell model was not evaluated during the 30% effort of Title I because the vertical spacing between cans and the can-supporting fixture design are still preliminary. The CDR vertical spacing between cans was 12 in., whereas recent values considered by Fluor Daniel and in the above facility analyses were 14.8 in. and 16.0 in. The can-supporting fixture design, which provides a significant heat-transfer path for cooling the plutonium storage containers, currently is a cylindrical 16-in.-diam metal plate, with or without holes, and with or without a conduction-path bridge to the drywell.

To provide a current estimate of the stored alpha-phase plutonium-metal maximum temperature, we will use the thermal results from a CFX4.1 drywell model[7] and a Thermal System Analysis Program triple-can British Nuclear Fuels Limited (BNFL) container on a 19-in.-diam plate storing the assumed worst-case two-plutonium-metal-buttons model.[8] The drywell-model case with a 12-in. vertical spacing between heated cans and no vertical thermal stratification of the vault air is considered appropriate for the Fluor-Daniel, Inc., facility air-temperature

distributions with heated cans in the bottom 80% of the drywell. From Figs. 6 and 11 in Ref. 7 for the hottest thirteenth can with a 15-W heat source, the temperature rise

- from the vault air to the drywell is 10.3°F (5.7 K),
- from the drywell to the drywell air is 10.4°F (5.8 K), and
- from the drywell air to the outer-can is 15.1°F (8.4 K).

The above results are for a 5-in.-diam can resting on an 8-in.-diam plate. For the 16-in.-diam fixture plate being considered in experiments by LANL group ESA-DE, the drywell-air-to-outer-can surface-average temperature rise would be a few degrees Fahrenheit less; therefore, using 15.1°F in our estimate is conservative. From Tables IV and V in Ref. 8 for the triple-can BNFL container on a 19-in.-diam plate, the temperature rise from the outer-can's surface-average temperature of 107.5°F (315.0 K) to the plutonium metal's maximum temperature in the upper button of 186.9°F (359.1 K) is 79.4°F (44.1 K). Adding all of the temperature changes to the LANL maximum 95.0°F (35.0°C, 308.1 K) ambient air temperature gives the plutonium metal's maximum temperature of 95.0 + (11.6 or 14.4) + 10.3 + 10.4 + 15.1 + 79.4 = 221.8°F (105.4°C, 378.6 K) for a 10,005-W heat source or 224.6°F (107.0°C, 380.2 K) for a 19,995-W heat source in the drywell-array vault. A double-can storage container would lower these temperatures by a few degrees Fahrenheit. Flat-bottomed storage cans on a 16-in.-diam plate would lower these temperatures greatly.

5.0. CONCLUSIONS

CFD modeling and analysis show the passive heat removal of the Fluor Daniel, Inc., NMSF renovation design (initial 30% of Title I) to be very good. Air flow down the drywell-array vault is uniform across the vault. There is a 50% decrease in the air velocity from the floor to the ceiling at the drywell-array inlet. The air velocity becomes vertically uniform at row 19 of the 47 drywell rows. To heat the air flow uniformly, the four drywells in a drywell row across the vault should be loaded uniformly with heated cans that are distributed preferentially toward the bottom of the drywell to avoid the lower air flow near the ceiling at the inlet and possible stratified hotter air near the ceiling at the outlet of the drywell array. With 10 heated cans per drywell occupying the lower 72% of the drywell vertical height, the maximum air-temperature change was only 12% to 17% above that for ideal uniform heating of the air for different heated-can loading patterns down the vault at 100% and 200% of the design heat load of 10,000 W. Lowering the heat load increased the nonuniformity of heating the vault air but decreased the maximum air temperature because the air flow per unit heat source is greater, which provides extra cooling. From four cases of different heat-source load, the volumetric air flow at the inlet to the facility as a function of the drywell-array vault total heat source was found to be predicted reasonably by the least-squares-fit functional-form volumetric air flow ($ft^3\ min^{-1}$) = 255.2 x [heat source (W)]$^{1/3}$. The maximum air temperature was predicted reasonably by the least-squares-fit functional form air temperature (°F) = 95.0 + 0.10

x [heat source (W)]$^{1/2}$. The 10,000-W design heat source per vault has a good volumetric air flow of ~5500 ft^3 min^{-1} and a maximum air-temperature change of ~10.4°F (5.8 K) from these formulas.

Undesirable air-flow swirls were found to occur under the sloped inlet ceiling and at the beveled top of the outlet stack. The sloped inlet ceiling air-flow swirls were primarily horizontal, with a lesser vertical swirl with the inlet tower on the side; they were primarily vertical with a lesser horizontal swirl with the inlet tower on the inlet end of drywell-array vault 1. The magnitude of these air-flow swirls (and their air-flow resistance) could be diminished by reducing the slope angle of the inlet ceiling (by extending it to the inlet edge of the drywell array). The air-flow swirl on the inlet-tower side of the beveled top of the outlet stack (that occurred in the facility calculations with volumetric air flows <5000 ft^3 min^{-1}) could be eliminated by reducing the angle of the bevel that expands the flow area from a 5-ft- to a 6.5-ft-diam circle over a 5-ft height.

Two cases that considered no-flow curtains in the drywell-array vault to establish vertical air flow only for the heated drywells showed that the curtains were not a viable concept for this facility design. The curtains would have to be designed for individual drywells to achieve that goal. In the process, the curtains provide a significant air-flow resistance, and without sufficient curtains, there are air-flow swirls and bypass air flow for the unheated drywells.

For the inlet tower with a volumetric air flow of 5500 ft^3 min^{-1} and no wind, adding the canopy and cruciform decreased the midtower pressure by 0.007 Pa (from -0.162 to -0.169 Pa). Adding the grilles decreased the midtower pressure by 0.042 Pa (from -0.169 to -0.211 Pa). Factoring in a west wind of 7.5 m s^{-1} (16.8 mph) increased the midtower pressure by 6.921 Pa (from -0.211 to 6.71 Pa). With the wind, there was counter-current air flow at the top of the tower and air-swirl vortices and cross air flow between grilles in the canopy-cruciform fixture.

The Fluor-Daniel facility-design-vault's maximum air-temperature change was 11.6°F (6.4 K) for a 10,005-W total heat source and 14.4°F (8.0 K) for a 19,995-W total heat source per vault. The maximum temperature change from the vault air to the maximum plutonium-metal temperature for the worst case of two plutonium-metal buttons stored in a triple-can BNFL container was estimated to be 115.2°F (64.0 K) from last year's drywell and container calculations. For a LANL maximum ambient air temperature of 95°F (308.2 K), the maximum plutonium-metal temperature is 221.8°F (105.4°C, 378.6 K) for a 10,005-W heat source and 224.6°F (107.0°C, 380.2 K) for a 19,995-W heat source in the drywell-array vault. These temperatures are less than the 284°F (140°C, 413 K) temperature limit for stored plutonium metal.

6.0. REFERENCES

1. R. G. Steinke, Los Alamos National Laboratory, personal communication with C. P. Ash, Fluor Daniel, Inc., March 1998.

2. I. E. Idelchik, *Handbook of Hydraulic Resistance* (Hemisphere Publishing Corporation, New York, 1986), 2nd Ed., pp. 407, 576.

3. R. G. Steinke, "Memo with NMSF Results from 12 CFX4.2 Calculations," TSA-10-98-140 memorandum to distribution (April 1998).

4. R. G. Steinke, "Memo with NMSF Results from a 13th CFX4.2 Calculation," TSA-10-98-146 memorandum to distribution (April 1998).

5. B. M. Bowen, "Los Alamos Climatology," Los Alamos National Laboratory report LA-11735-MS, p. 90 (May 1990).

6. C. Müller, "Memo with NMSF Inlet-Tower Results from 4 CFX4.2 Calculations," TSA-10-98-156 memorandum to distribution (May 1998).

7. R. G. Steinke, "Thermal Analysis of the Drywell for the Nuclear Material Storage Facility," Los Alamos National Laboratory report LA-UR-97-118 (January 1997).

8. T. D. Knight and R. G. Steinke, "Thermal Analyses of Plutonium Materials in British Nuclear Fuels, Ltd., Containers," Los Alamos National Laboratory report LA-UR-97-1866 (June 1997).

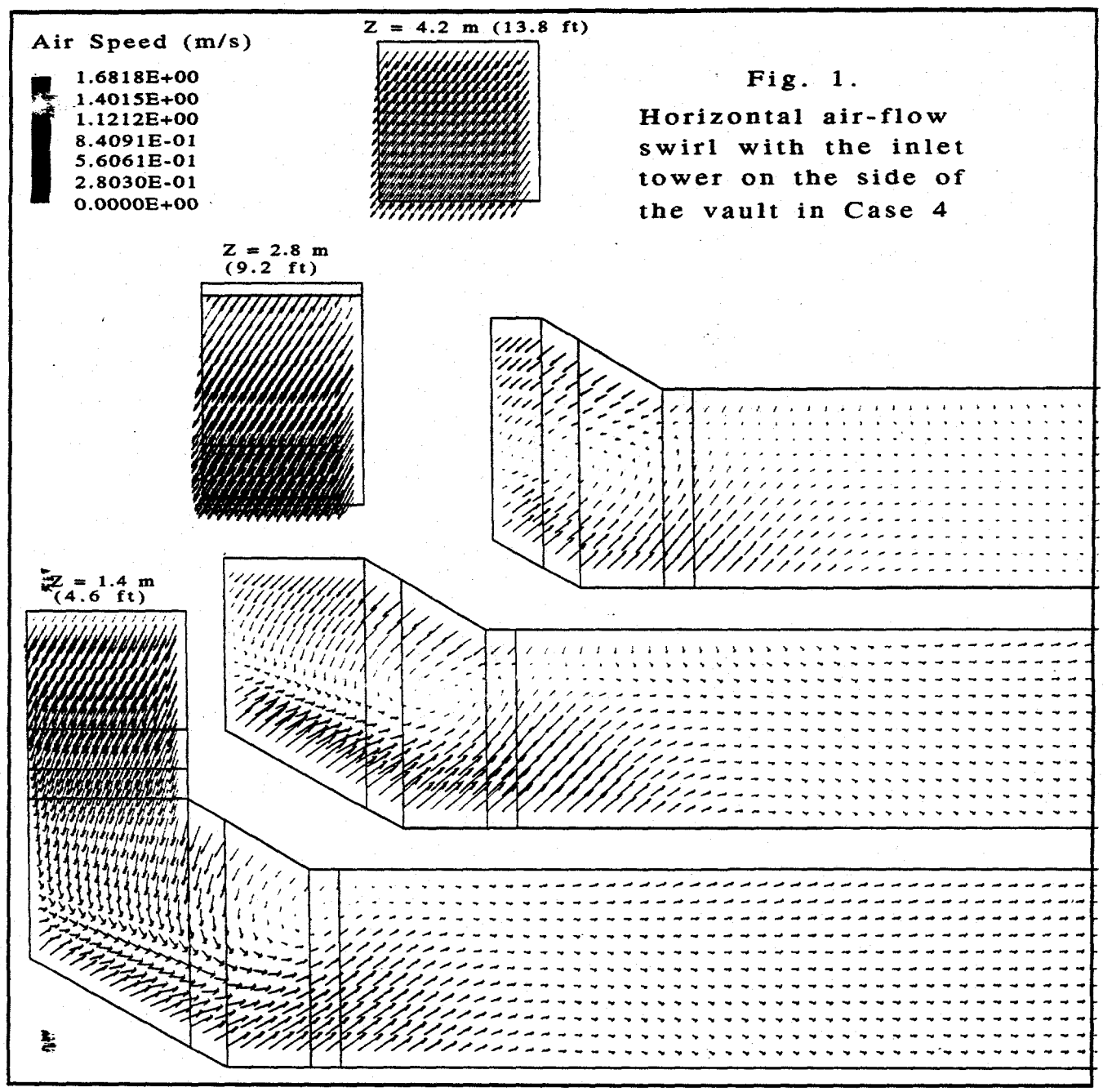

Fig. 1.
Horizontal air-flow swirl with the inlet tower on the side of the vault in Case 4

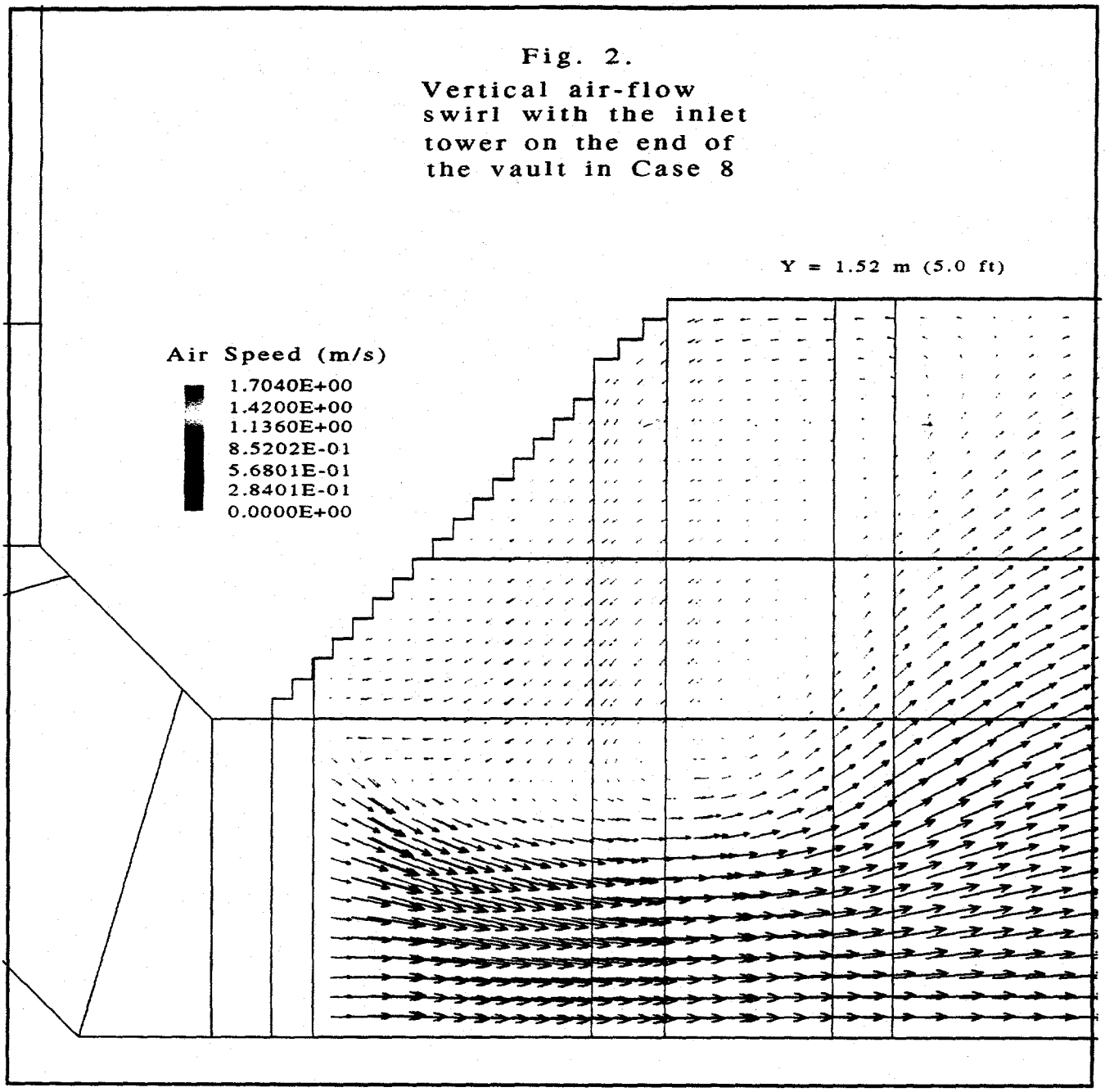

Fig. 2.
Vertical air-flow swirl with the inlet tower on the end of the vault in Case 8

Fig. 3.
Air Temperature from the heated drywells in drywell rows 1 to 17 of Case 4

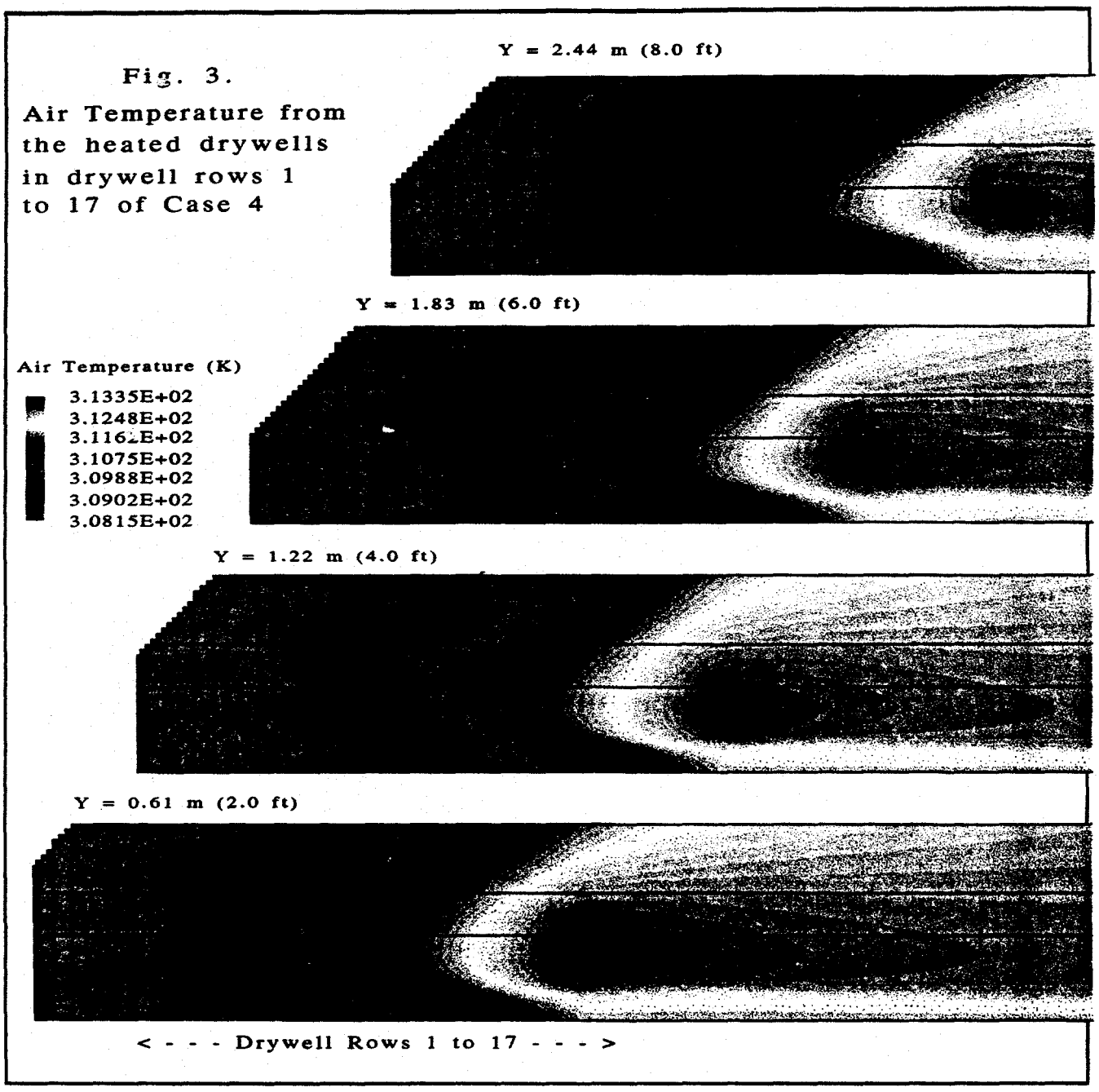

Fig. 3.
Air Temperature from the heated drywells in drywell rows 1 to 17 of Case 4

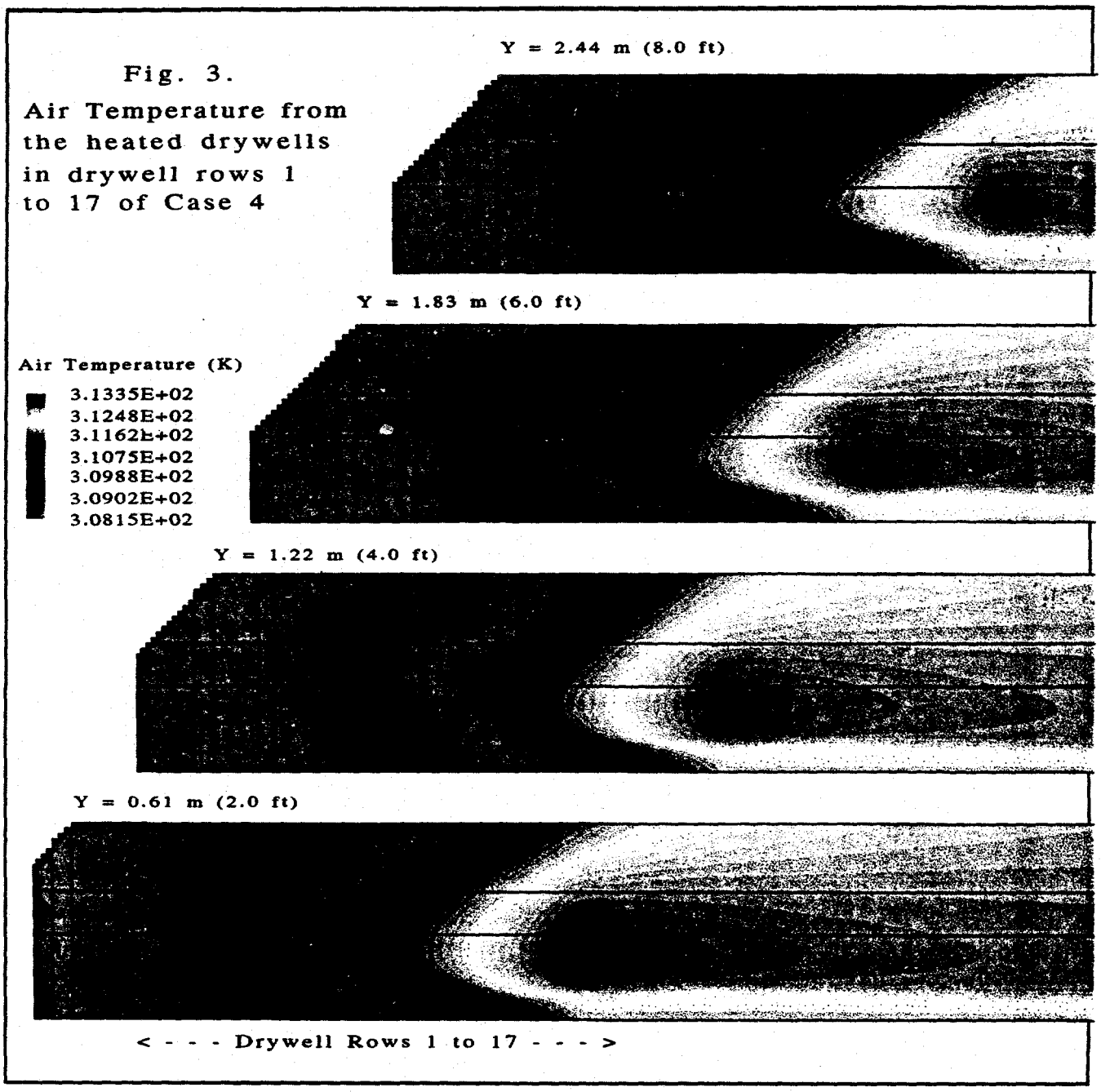

Fig. 4. Air Flow in Inlet Tower

Design Case with Canopy, Cruciform and Grilles
Cut through Y plane 0.4656 m away from center of cruciform

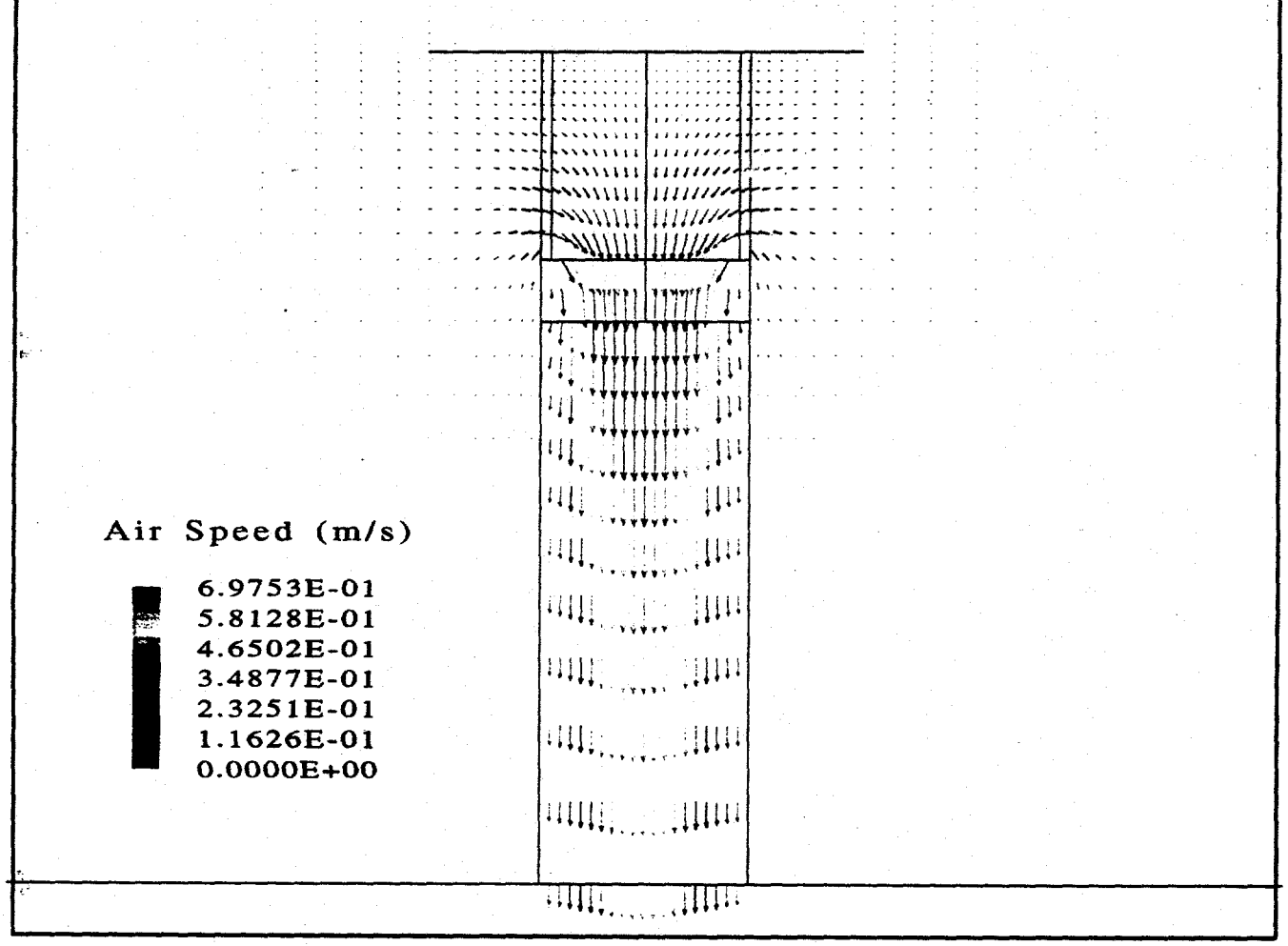

Fig. 5. Pressure in Inlet Tower

Design Case with Canopy, Cruciform and Grilles
Cut through Y plane 0.4656 m away from center of cruciform